First demonstration of SiGe-based carrier-injection Mach-Zehnder modulator with enhanced plasma dispersion effect

Younghyun Kim,[1,*] Junichi Fujikata,[2] Shigeki Takahashi,[2] Mitsuru Takenaka,[1] and Shinichi Takagi[1]

[1]*Dept. of Electrical Engineering and Information Systems, The University of Tokyo 7-3-1 Hongo, Bunkyo-ku, Tokyo 113-0032, Japan*

[2]*Photonics Electronics Technology Research Association (PETRA), 16-1, Onogawa, Tsukuba 305-8569, Japan*

[*]*yhkim@mosfet.t.u-tokyo.ac.jp*

Abstract: We demonstrate a strained $Si_{0.91}Ge_{0.09}$-based carrier-injection Mach-Zehnder (MZ) optical modulator using the enhanced plasma dispersion effect in strained SiGe through mass modulation for the first time. The SiGe modulator has an injection current of 1.47 mA for a phase shift of π which is lower than that for a Si modulator. Also, it is expected that the injection current can be further reduced by increasing the strain and Ge fraction, enabling operation at an injection current of less than 1 mA. As an example of the dynamic characteristics, 10 Gbps modulation with clear eye opening was obtained by the pre-emphasis method.

OCIS codes: (130.3120) Integrated optics devices; (250.7360) Waveguide modulators.

References and links

1. G. T. Reed, G. Mashanovich, F. Y. Gardes, and D. J. Thomson, "Silicon optical modulators," Nat. Photonics **4**(8), 518–526 (2010).
2. Q. Xu, B. Schmidt, S. Pradhan, and M. Lipson, "Micrometre-scale silicon electro-optic modulator," Nature **435**(7040), 325–327 (2005).
3. Y. H. Kuo, Y. K. Lee, Y. Ge, S. Ren, J. E. Roth, T. I. Kamins, D. A. B. Miller, and J. S. Harris, "Strong quantum-confined Stark effect in germanium quantum-well structures on silicon," Nature **437**(7063), 1334–1336 (2005).
4. J. Liu, M. Beals, A. Pomerene, S. Bernardis, R. Sun, J. Cheng, L. C. Kimerling, and J. Michel, "Waveguide-integrated, ultralow-energy GeSi electro-absorption modulators," Nat. Photonics **2**(7), 433–437 (2008).
5. W. M. J. Green, M. J. Rooks, L. Sekaric, and Y. A. Vlasov, "Ultra-compact, low RF power, 10 Gb/s silicon Mach-Zehnder modulator," Opt. Express **15**(25), 17106–17113 (2007).
6. L. Liao, A. Liu, D. Rubin, J. Basak, Y. Chetrit, H. Nguyen, R. Cohen, N. Izhaky, and M. Paniccia, "40 Gbit/s silicon optical modulator for high-speed applications," Electron. Lett. **43**, 51–52 (2009).
7. F. Y. Gardes, D. J. Thomson, N. G. Emerson, and G. T. Reed, "40 Gb/s silicon photonics modulator for TE and TM polarisations," Opt. Express **19**(12), 11804–11814 (2011).
8. D. J. Thomson, F. Y. Gardes, J. M. Fedeli, S. Zlatanovic, Y. F. Hu, B. P. P. Kuo, E. Myslivets, N. Alic, S. Radic, G. Z. Mashanovich, and G. T. Reed, "50-Gb/s silicon optical modulator," IEEE Photonics Technol. Lett. **24**(4), 234–236 (2012).
9. M. Liu, X. Yin, E. Ulin-Avila, B. Geng, T. Zentgraf, L. Ju, F. Wang, and X. Zhang, "A graphene-based broadband optical modulator," Nature **474**(7349), 64–67 (2011).
10. M. Liu, X. Yin, and X. Zhang, "Double-layer graphene optical modulator," Nano Lett. **12**(3), 1482–1485 (2012).
11. A. V. Krishnamoorthy, X. Zheng, D. Feng, J. Lexau, J. F. Buckwalter, H. D. Thacker, F. Liu, Y. Luo, E. Chang, P. Amberg, I. Shubin, S. S. Djordjevic, J. H. Lee, S. Lin, H. Liang, A. Abed, R. Shafiiha, K. Raj, R. Ho, M. Asghari, and J. E. Cunningham, "A low-power, high-speed, 9-channel germanium-silicon electro-absorption modulator array integrated with digital CMOS driver and wavelength multiplexer," Opt. Express **22**(10), 12289–12295 (2014).
12. T. Baehr-Jones, R. Ding, Y. Liu, A. Ayazi, T. Pinguet, N. C. Harris, M. Streshinsky, P. Lee, Y. Zhang, A. E. J. Lim, T. Y. Liow, S. H. G. Teo, G. Q. Lo, and M. Hochberg, "Ultralow drive voltage silicon traveling-wave modulator," Opt. Express **20**(11), 12014–12020 (2012).
13. J. F. Ding, R. Q. Ji, L. Zhang, and L. Yang, "Electro-optical response analysis of a 40 Gb/s silicon Mach-Zehnder optical modulator," J. Lightwave Technol. **31**(14), 2434–2440 (2013).
14. M. Takenaka and S. Takagi, "Strain engineering of plasma dispersion effect for SiGe optical modulators," IEEE J. Quantum Electron. **48**(1), 8–16 (2012).

#253968 Received 16 Nov 2015; revised 18 Dec 2015; accepted 23 Dec 2015; published 25 Jan 2016

15. Y. Kim, M. Takenaka, T. Osada, M. Hata, and S. Takagi, "Strain-induced enhancement of plasma dispersion effect and free-carrier absorption in SiGe optical modulators," Sci. Rep. **4**, 4683 (2014).
16. Y. Kim, J. Fujikata, S. Takahashi, M. Takenaka, and S. Takagi, "Demonstration of record-low injection-current variable optical attenuator based on strained SiGe with optimized lateral pin junction," Opt. Express **23**(9), 12354–12361 (2015).
17. Y. Kim, M. Takenaka, T. Osada, M. Hata, and S. Takagi, "Fabrication and evaluation of propagation loss of Si/SiGe/Si photonic-wire waveguides for Si based optical modulator," Thin Solid Films **557**, 342–345 (2014).
18. P. Dong, S. Liao, H. Liang, R. Shafiiha, D. Feng, G. Li, X. Zheng, A. V. Krishnamoorthy, and M. Asghari, "Submilliwatt, ultrafast and broadband electro-optic silicon switches," Opt. Express **18**(24), 25225–25231 (2010).
19. G. R. Zhou, M. W. Geis, S. J. Spector, F. Gan, M. E. Grein, R. T. Schulein, J. S. Orcutt, J. U. Yoon, D. M. Lennon, T. M. Lyszczarz, E. P. Ippen, and F. X. Käertner, "Effect of carrier lifetime on forward-biased silicon Mach-Zehnder modulators," Opt. Express **16**(8), 5218–5226 (2008).
20. J. Van Campenhout, W. M. J. Green, S. Assefa, and Y. A. Vlasov, "Low-power, 2 x 2 silicon electro-optic switch with 110-nm bandwidth for broadband reconfigurable optical networks," Opt. Express **17**(26), 24020–24029 (2009).
21. D. V. Lang, R. People, J. C. Bean, and A. M. Sergent, "Measurement of the band gap of GexSi1-x/Si strainedlayer heterostructures," Appl. Phys. Lett. **47**(12), 1333–1335 (1985).
22. J. Fujikata, M. Miura, M. Noguchi, D. Okamoto, T. Horikawa, and Y. Arakawa, "Si Waveguide-Integrated Metal–Semiconductor–Metal and p–i–n-Type Ge Photodiodes Using Si-Capping Layer," Jpn. J. Appl. Phys. **52**(4S), 04CG10 (2013).
23. Q. Xu, S. Manipatruni, B. Schmidt, J. Shakya, and M. Lipson, "12.5 Gbit/s carrier-injection-based silicon micro-ring silicon modulators," Opt. Express **15**(2), 430–436 (2007).

1. Introduction

There have been great achievements in the development of Si-based optical modulators, which are a key component for high-speed and low-power optical interconnects, particularly for data center networks [1–11]. Among the various types of Si-based optical modulators reported so far, carrier-depletion-type Si Mach-Zehnder (MZ) optical modulators based on the plasma dispersion effect have mostly been demonstrated for high-speed modulation and broad-wavelength operation. However, a carrier-depletion Si modulator requires a relatively long phase shifter or a high driving voltage owing to its low modulation efficiency caused by the weak plasma dispersion effect in Si [12, 13]. This is unfavorable for large-scale integration in terms of a small footprint, low driving voltage, and low power consumption. To further improve in the modulation efficiency, we have proposed strained SiGe technology for modulators, variable optical attenuators, and switches. The free-carrier effects of the plasma dispersion effect and free-carrier absorption are theoretically expected to be enhanced by reducing the effective mass of holes in strained SiGe because these effects are inversely proportional to the effective mass of carriers according to the Drude model [14]. Furthermore, we have reported experimental demonstrations of the enhanced free-carrier effects in strained SiGe [15] and low-power SiGe variable optical attenuators (VOAs) [16]. However, the enhancement of the plasma dispersion effect in SiGe was obtained from the Kramers-Kronig relationship through the experimentally obtained absorption spectrum using a VOA in the previous work [15]. In other words, the enhancement of the plasma dispersion effect in strained SiGe has not been directly measured through the change in the effective refractive index using an interferometer. Therefore, it is necessary to demonstrate SiGe MZ optical modulators based on the enhanced plasma dispersion effect.

In this paper, we demonstrate a SiGe MZ optical modulator with higher modulation efficiency than a Si modulator owing to the enhanced plasma dispersion effect in strained SiGe for the first time. We also show 10 Gbps modulation with clear eye opening by the carrier-injection type SiGe MZ modulator by pre-emphasis driving.

2. Numerical analysis of SiGe MZ modulator

To estimate the improvement in the modulation efficiency by taking into account the strain-induced enhancement of the plasma dispersion effect in SiGe, we numerically analyzed a carrier-injection strained SiGe MZ modulator with a lateral p-i-n junction by technology computer-aided design simulation (Sentaurus) and finite-difference optical mode analysis [15]. Figure 1(a) shows the device structure of the phase shifter in the SiGe MZ modulator,

#253968 Received 16 Nov 2015; revised 18 Dec 2015; accepted 23 Dec 2015; published 25 Jan 2016

which consists of 40-nm-thick SiGe in the waveguide core and a lateral p-i-n junction. Figure 1(b) shows the calculated change in the effective refractive index as a function of the injected carrier density for various Ge fractions in SiGe from 0.0 to 0.3. With increasing injection current, the change in the effective refractive index increases owing to the plasma dispersion effect. When the Ge fraction increases, the change in the effective refractive index also becomes larger owing to the enhanced plasma dispersion effect in strained SiGe. Hence, the injection current required for a phase shift of π decreases with increasing Ge fraction as shown in Fig. 1(c). Note that the injection current can be as low as 0.7 mA using $Si_{0.7}Ge_{0.3}$ in the case of a 250-μm-long phase shifter, approximately 2.5 times lower than the current required for a phase shift of π in a Si device.

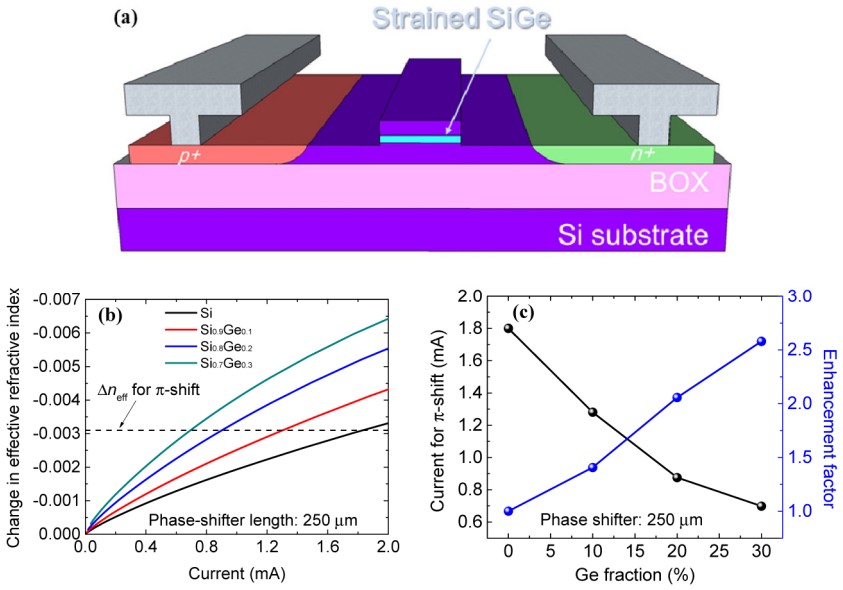

Fig. 1. (a) Device structure of the phase shifter in the carrier-injection SiGe MZ modulator, (b) simulation result for change in effective refractive index as a function of injected current density with Ge fractions from 0.0 to 0.3 when the phase-shifter length is 250 μm, and (c) current density required for a phase shift of π (left axis) and its enhancement factor (right axis) as a function of Ge fraction.

2. Fabrication of strained SiGe MZ modulator

We fabricated the SiGe asymmetric MZ modulator with a conventional Si CMOS process. First, a 45-nm-thick pseudomorphic $Si_{0.86}Ge_{0.14}$ layer and a 75-nm-thick Si layer were grown on a105-nm-thick silicon-on-insulator (SOI) by chemical vapor deposition (CVD). Secondly, 600-nm-wide waveguides with a Si/SiGe/Si core were formed by electron beam lithography and reactive ion etching with CF_4. Then, the ion implantation of boron and phosphorus was implemented to form p-i-n junctions. To reduce the sidewall scattering loss, annealing in O_2 atmosphere was also performed in the middle of activation annealing in N_2 atmosphere. Although the Ge fraction of the SiGe layer was changed from 14% to 9% as a result of Ge diffusion during the activation annealing, the strain in the SiGe was almost maintained [15]. Finally, an Al electrode was formed by thermal evaporation followed by forming gas annealing at 400 °C. We also simultaneously prepared a Si asymmetric MZ modulator using a 220-nm-thick SOI as a reference device. Figure 2(a) shows a top view of the SiGe asymmetric MZ modulator taken by optical microscopy, which consists of two 1 × 2 multimode interference (MMI) couplers and 250-μm-long phase shifters in the two MZ interferometer arms. Figure 2(b) shows a tilted SEM image of the fabricated device. Figures 2(c) and 2(d) show the well-defined 1 × 2 MMI coupler and bent Si/SiGe/Si waveguide, respectively.

#253968 Received 16 Nov 2015; revised 18 Dec 2015; accepted 23 Dec 2015; published 25 Jan 2016

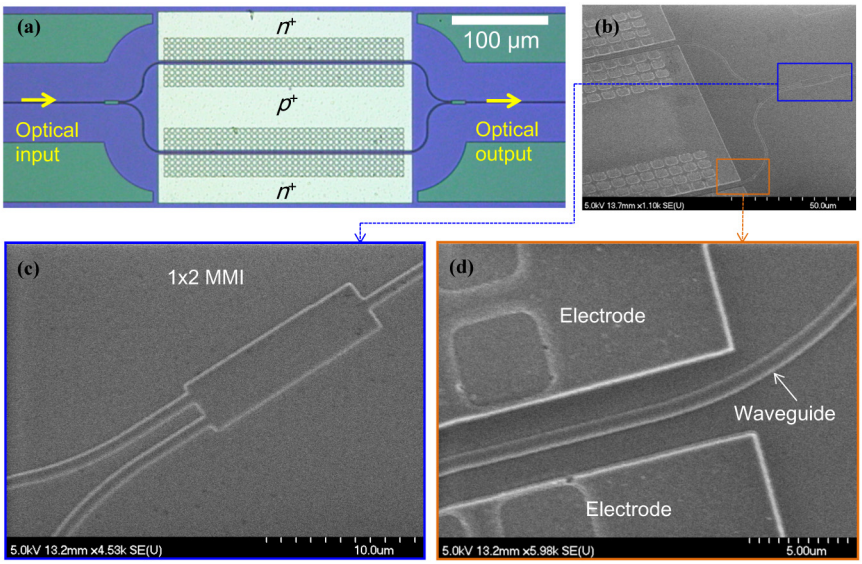

Fig. 2. (a) Optical microscopy image of the SiGe asymmetric MZ modulator, (b) tilted SEM image of the device, (c) well-defined 1 × 2 MMI coupler, and (d) bent Si/SiGe/Si waveguide.

3. Static characteristics of strained SiGe asymmetric MZ modulator

First we evaluated the electrical characteristics of the lateral p-i-n junctions. Figures 3(a) and 3(b) show the *I-V* characteristics of the lateral p-i-n junctions in the 250-μm-long phase shifters of the Si and SiGe modulators plotted on log and linear scales, respectively. It is shown in Figs. 3 that the threshold voltage of the SiGe modulator is smaller than that of the Si modulator owing to the reduction in the built-in potential by the strained SiGe. Therefore, low-power operation is expected as a result of the low threshold voltage in the strained SiGe device. Additionally, the crossover in the injection current is due to the higher Auger recombination rate in SiGe for high-injection region.

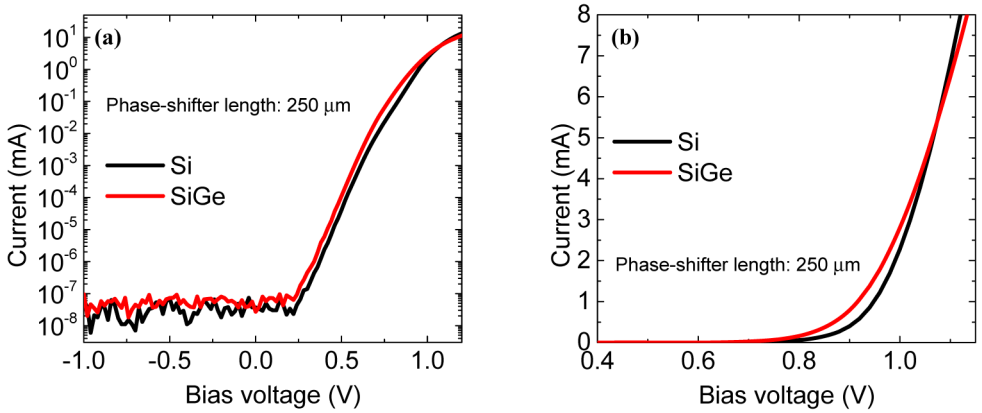

Fig. 3. *I-V* characteristics of the lateral p-i-n junctions in the Si and SiGe devices on (a) logarithmic and (b) linear scales.

We evaluated the phase shift in the SiGe and Si asymmetric MZ modulators by measuring the change in the wavelength spectrum while injecting current through the p-i-n junction. The amounts of power dissipation for the π phase shift are approximately 1.8 mW for the Si device and 1.4 mW for the SiGe devices, respectively. Thus, the difference in the power

#253968 Received 16 Nov 2015; revised 18 Dec 2015; accepted 23 Dec 2015; published 25 Jan 2016

dissipation is approximately 0.4 mW. We analyzed the temperature change in the Si phase-shifter as a function of power consumption by COMSOL. The temperature change is less than 1 K even when the power dissipation is a few mW. Furthermore, we used the thermal controller to maintain the temperature of sample stage constant to avoid the thermal effect. Thus, the thermal effect is negligible in our experiments. Continuous-wave TE-polarized light in the wavelength range of 1530 to 1590 nm was coupled to the cleaved waveguide facet through a lensed fiber. Then, the output power was monitored using an InGaAs photodetector. The free spectrum range of the asymmetric MZ interferometer was designed to be approximately 30 nm via a 20 μm difference in the length between the two MZI arms. Figures 4(a) and 4(b) show the transmission spectra of the Si and SiGe modulators with injection currents of 0 mA and 2 mA, respectively. The wavelength spectra are shifted by the increase in the optical phase difference between the two MZI arms owing to the plasma dispersion effect. The phase shift was extracted from these shifts in the spectra. In terms of insertion loss, the propagation loss caused by the free-carrier absorption is not significant even in the SiGe device when the injection current is less than 2 mA. From the numerical analysis, we expect the difference in the insertion loss between the Si and SiGe devise is less than 1 dB. The bandgap narrowing in SiGe may cause the increase in the propagation loss especially in the case of Ge-rich SiGe. In our previous work [17], we evaluated the propagation loss of a SiGe waveguide, which is similar structure to this study. Even the SiGe has the higher Ge fraction of 28%, the propagation loss is 0.54 dB/mm. In this study, the Ge fractions is 9%, therefore, we could not observe a significant insertion loss increase in the SiGe device. In fact, the insertion loss in the Si device was higher than that in the SiGe device. In Fig. 4, the maximum output power can be considered as the insertion loss, which is around – 30 dB for the SiGe device and – 37 dB for the Si device. It might be caused by dry etching process, which is not essential issue for this paper.

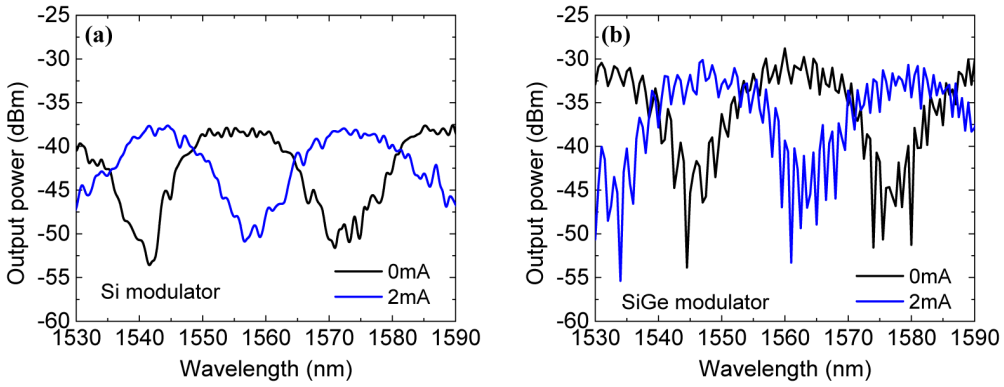

Fig. 4. Measured transmission spectra with injection currents of 0 mA and 2 mA in (a) Si and (b) SiGe asymmetric MZ modulators.

Figure 5(a) shows the optical phase shift of the Si and SiGe asymmetric modulators as a function of the injected current, obtained from the wavelength spectrum at each injected current as shown in Figs. 4. The optical phase shift increases with increasing injection current owing to the plasma dispersion effect. The SiGe modulator exhibits a higher optical phase shift than the Si modulator at the same injection current, indicating that the modulation efficiency is improved by the enhancement of the plasma dispersion effect in strained SiGe. The injection currents for a phase shift of π are 1.47 mA for the SiGe modulator and 1.87 mA for the Si modulator with the 250-μm-long phase shifter. Additionally, the $V_{\pi}L$ are 0.0235 Vcm for the SiGe modulator and 0.0245 Vcm for the Si modulator. The Fabry-Pérot resonance especially observed in Fig. 4(b) might degrade the accuracy in the phase shift evaluation. We estimate that the error in the peak wavelength measurement caused by the Fabry-Pérot resonance is approximately 1 nm, resulting in less than 5% error in the phase

#253968 Received 16 Nov 2015; revised 18 Dec 2015; accepted 23 Dec 2015; published 25 Jan 2016

shift evaluation when the injection current is 2.5 mA. Therefore, the phase shift difference between the SiGe and Si devices is fairly evaluated.

Figure 5(b) shows benchmark injection currents, required for a phase shift of π in the carrier-injection phase shifter as a function of the phase-shifter length. A larger injection current is required to obtain a phase shift of π when the phase-shifter length is reduced [18]. Among the Si modulators reported so far [18–20], the Si modulator in this work exhibits one of the lowest injection currents in the case of a 250-μm-long phase shifter, which may be attributable to the optimized fabrication procedure of the p-i-n junction. As shown in Fig. 5(b), further reduction in the injection current is achieved using the SiGe optical modulator. The open circles in Fig. 5(b) show the simulated injection currents for a phase shift of π for the Ge fractions from 0 to 0.3, obtained by the numerical analysis of SiGe modulators. It was found that the experimental results for the Si and SiGe modulators show relatively good agreement with the simulation results. Thus, it is highly expected that the injection current for a phase shift of π can be reduced to less than 1 mA by using a higher strain and Ge fraction.

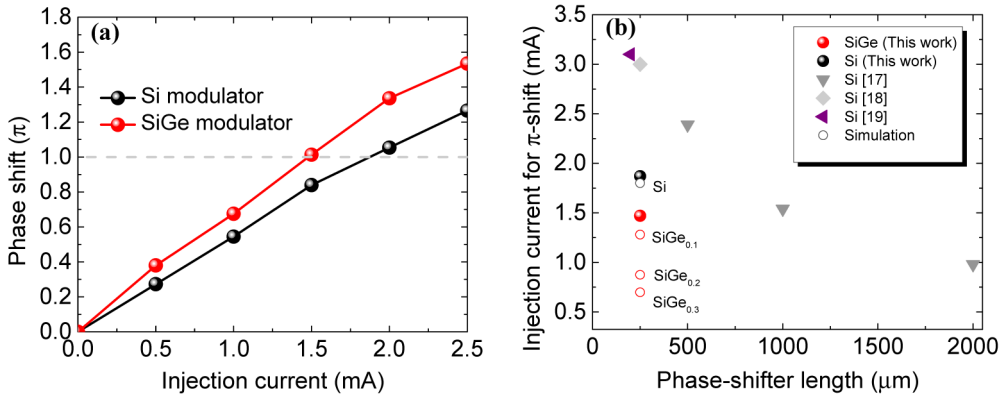

Fig. 5. (a) Extracted phase shift as a function of injection current for Si and SiGe asymmetric MZ modulators, and (b) benchmark injection currents for a phase shift of π as a function of phase-shifter length.

In terms of upper limit of Ge fraction, the loss should be considered. The loss by bandgap absorption becomes dominant as increasing Ge fraction. In case of strained SiGe, the loss dramatically increases because the bandgap rapidly decrease with Ge fraction [21]. Therefore, the maximum Ge mole fraction in bulk SiGe is approximately 30% to avoid the bandgap absorption. The Ge fraction up to 50% is acceptable in the case of the SiGe quantum well [14]. The insertion loss due to SiGe can be further reduced by the selective growth of SiGe only on the phase shifter waveguides as the Ge selective growth on a recessed Si waveguide reported in [22]. Also, it is expected to reduce nonlinear optical phenomena such two-photon absorption.

4. Dynamic characteristics

We performed the high-speed modulation of the SiGe asymmetric MZ modulator under the measurement setup in Fig. 6(a). A 10 Gbps non-return-to-zero (NRZ) $2^7 - 1$ pseudo-random bit sequence (PRBS) electrical signals were converted to the pre-emphasis signals using differentiators [23]. We expect that the error rate will increase when the PRBS patterns of $2^{15} - 1$ and $2^{31} - 1$ because the low frequency response cannot be compensated well by the single differentiator used in this experiment to generate the pre-emphasis signal. However, the error-free operation can be expected even for the PRBS patterns of $2^{15} - 1$ and $2^{31} - 1$ optimizing the pre-emphasis signal. Then, the electrical signals with a peak-to-peak voltage of 2.1 V and a dc voltage of – 0.78 V were applied to both arms of the SiGe modulator for push-pull operation. As shown in Fig. 6(b), clear eye opening at 10 Gbps was successfully obtained at a wavelength of 1541 nm, which corresponds to a balance point of –3 dB. In our test setup, we

#253968 Received 16 Nov 2015; revised 18 Dec 2015; accepted 23 Dec 2015; published 25 Jan 2016

cannot directly evaluate the extinction ratio from the eye pattern. However, we expect the extinction ratio of approximately 4 dB by comparing to the eye pattern of the calibrated optical signal with a 4 dB extinction ratio.

In terms of small signal response, we demonstrated the comparison between Si and SiGe device in our previous work [16]. The 3 dB bandwidth is 246 MHz for the SiGe device and 161 MHz for the Si device, respectively. The SiGe device seems to have approximately 1.5 times greater bandwidth than the SiGe device due to the higher Auger recombination rate in the SiGe layer.

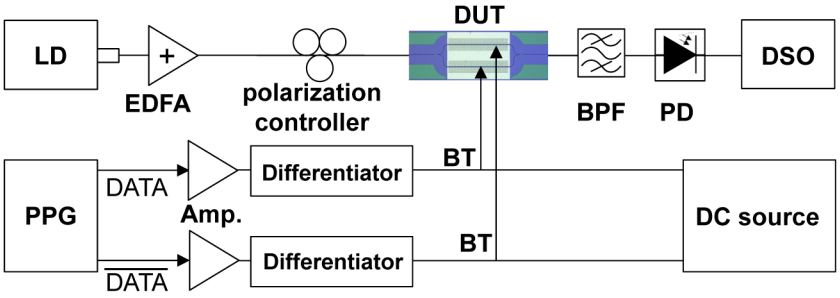

(a)

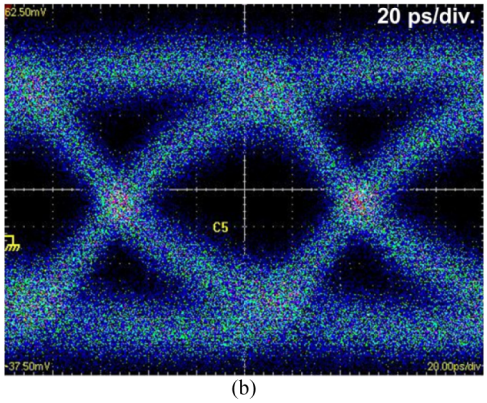

(b)

Fig. 6. (a) Measurement setup used to obtain dynamic characteristics of SiGe modulator, and (b) eye pattern of SiGe MZ modulator at 10 Gbps.

6. Conclusion

We have demonstrated a SiGe-based MZ optical modulator with a p-i-n lateral diode for carrier injection. The enhanced plasma dispersion in strained SiGe was experimentally observed for the first time. The injection current required for a phase shift of π is reduced to 1.47 mA, compared with 1.87 mA for a Si modulator. It is also expected that the modulation efficiency can be further improved by using a higher strain and Ge fraction, enabling operation at an injection current of less than 1 mA. A 10 Gbps clear eye pattern was also successfully obtained by the pre-emphasis method. In this study, we used asymmetric MZM to figure out the enhancement of the plasma dispersion effect in SiGe, A symmetric MZM can also be demonstrated with strained SiGe, taking advantage of its large optical bandwidth. Therefore, strained SiGe is a highly promising material for the further development of Si-based optical modulators.

Acknowledgments

This work was supported in part by NEDO in "Integrated Photonics-Electronics Convergence System Technology (PECST)".

#253968 Received 16 Nov 2015; revised 18 Dec 2015; accepted 23 Dec 2015; published 25 Jan 2016